SI Appendix Material and Methods (Analysis of human samples)

Immunohistochemistry (IHC)

Breast preneoplastic and tumor tissues were obtained from women carrying BRCA1/2 mutations. Control breast tissue samples were acquired from anonymous premenopausal women undergoing reduction mastectomy at the University Hospital of Bellvitge, IDIBELL. IHC was performed as previously described(1). Tissue samples were incubated overnight at 4ºC with anti-amphiregulin primary Ab (16036-1 AP, Proteintech) at a dilution of 1:100. Specimens were viewed with a brightfield microscope (Leica DM2500 equipped with Micropublisher 3.3-QI imaging camera) using Q-Capture Pro Software and processed with Adobe Photoshop CS5.

For identification of human CD163-positive macrophages in human breast cancers, IHC was performed with CD163 primary antibody (MCA1853, Bio-Rad) as previously described(2). AREG positive regions were identified by pre-segmenting the images at 10x magnification using multiresolution segmentation in Definiens DeveloperXD (scale = 800, shape coefficient = 0.4, compactness coefficient = 0.1) and classified based on the object's mean intensity, the number of standard deviations from the image mean in AREG stain channel, its relative brightness compared to neighbour objects, and with shape morphometrics. AREG positive regions were grown by 20 pixels (~26um) up to 100 pixels in order to fill gaps between very close AREG positive objects, to include immediately adjacent stroma, and to combine small regions of AREG positive epithelium that, in a 3D setting, would have come from the same structure. AREG negative regions were identified as any regions which was not AREG positive or one of the pixel-distance bins. Any misclassified regions were manually corrected. Images were captured with Olympus IX81 fluorescence microscope and processed with ZEN imaging software, CZI. Data were analyzed by GraphPad Prism 7.

For IHC staining of mouse KBP tumors, tissue specimens were incubated with primary Abs to detect amphiregulin (16036-1 AP, Proteintech), F4/80 (MCA497GAR, Bio-Rad), and CD31(AB28364, Abcam). For amphiregulin, we applied the same conditions as for human breast cancer specimen as described above. For F4/80 staining, antigen retrivial for perfomed with Proteinase K (PK) treatment at 37°C for 10 min. The primary Ab was prepared in 5% rabbit serum with 0,2% Triton X-100 at a dilution of 1:200 overnight at

4ºC. Secondary Ab (Vector labs BA-4001) was incubated for 30 min at a dilution of 1:400. For IHC staining of CD31 positive cells tissue samples were incubated in 10mM Na Citrate (pH6) solution. The primary Ab was diluted at 1:50 dilution in DAKO Protein block and incubated for 45 minutes at room temperature. Secondary Ab (Jackson Labs) was diluted 1:400 and incubated for 45 minutes. In both cases, slides were digitized using a Nanozoomer2.0 HT-Hamamatsu (Olympus). An image analysis protocol (APP) was developed using Visiopharm software (Visiopharm, Denmark) to identify the area of IHC staining positive for F480 and CD31. A ratio of positive expression to region of interest was then calculated for each test group. In both human breast cancer and mouse tumor specimen, DAPI was used as nuclear staining.

Analysis of human breast cancer datasets

The results published here are partly based upon data generated by TCGA managed by the National Cancer Institute (NCI) and the National Human Genome Research Institute (NHGRI). Information about TCGA can be found at http://cancergenome.nih.gov. HR-deficient BC cohort was defined by using TCGA breast cancer RNAseq data and somatic mutations after being obtained following approval by the Data Access Committee (project #11689). Mutational signatures were defined using the R mut Signatures package(3). The GSEA tool was run with default values for all parameters.

Gene expression differences stratified according to BRCA1 mRNA level were analyzed using preprocessed and normalized RNA-seq and microarray expression TCGA data (downloaded from the GDC data portal on 2016-04-22). For each gene, a logistic regression analysis was implemented to assess its association with the expression level of BRCA1, categorized in tertiles. Unadjusted and adjusted (with covariates of ERBB2, ESR1, and PGR expression) models were used, which provided similar estimations. Gene expression correlations were computed using Pearson's correlation coefficient, and p-values indicated the probability of independence. Data were normalized to log2 standard TCGA normalization. Rosetta microarray-derived gene expression data along with BRCA1 mutation status from the Van't Veer cohort were downloaded from http://www.rii.com/publications/default.htm(4). Because the expression profiles obtained were log-ratio data, no further normalization was performed. Comparison of AhR, CYP1A1, and CYP1A2 expression levels in BRCA1-mutated versus wild-type breast

tumors was performed using a two-tailed Mann-Whitney U test and GraphPad Prism Software.

PAM50 calls annotated in clinical data were used to identify primary breast tumors of the basal subtype (n=141) which were segregated into quartiles based on *AREG* mRNA levels. Candidate gene expression levels were then compared in tumors in the top and bottom quartiles. Expression profiles were subjected to single sample gene set enrichment analysis (ssGSEA) using the Broad's GenePattern tool to derive individual tumor enrichment scores for a panel of MSigDB gene-sets corresponding to the cellular response to oxidative stress (http://software.broadinstitute.org/cancer/software/genepattern/)(5, 6). The "Chuang_oxidative_stress_response" gene set (ROS up-regulated genes only) displayed the greatest variance in ssGSEA enrichment scores across tumors and was chosen for subsequent analysis. Tumors were classified into quartiles based on their ssGSEA scores for this gene-set. AhR, CYP1B1, AREG, CCL5, CXCL1 and CXCL2 expression levels were then compared between tumors in the top and bottom quartiles, representing those with high and low responses to oxidative stress, respectively. All two-group statistical comparisons of gene expression levels were performed using a two-tailed Mann-Whitney U test and GraphPad Prism Software.

The immune cell content in tumors was inferred using the Microenvironment Cell Populations-counter method (7). These analyses and PCC computations were performed in R software.

The AHR and AHR-ARNT target gene sets were obtained from the TRANSFAC database(8). The expression signature scores were computed using the ssGSEA algorithm with standard parameters and using all genes included in each set. The Pearson's correlation coefficients and p-values were computed in R.

Cancer Cell Line Encyclopedia was used to investigate the expression of AhR in human breast cancer cell lines(9, 10). The cell lines were grouped into basal-like and non-basal-like based on the method previously described(11).

SI Appendix Figure Legends

Figure S1. **AhR expression and activation in NRF2-deleted cells and BC with high ROS levels.** (*A)* AhR mRNA levels in human MCF10A cells left untreated (Ctr) or treated with 200μM BSO for 24h. (*B*) Representative images of immunofluorescence assay in COMMA-1D cells treated with 200μM BSO for 1h or left untreated (Ctr). Blue=nuclear staining with Dapi, Magenta=AhR staining. The cells contained in dashed rectangles are reported in Figure 1*D* as example of scoring criteria of low/undetectable or positive AhR nuclear signal. Scale bar=20μm. (*C*) Expression levels of Ahr exon2 in mouse MEC that were isolated from $Ahr^{f/f}$ mice, infected with cre-expressing (+cre) or empty vector (-cre) adenoviruses and then left untreated (Ctr) or treated with 50 μM BSO for 24hr before analysis. (*D*) Nrf2 mRNA levels of mouse MEC isolated from $Nrf2^{-/-}$ or $Nrf2^{+/+}$ mice. (*E*) AhR mRNA levels of mouse MEC as in (*D*). (*F*, *G*) Hmox1 and Nqo1 mRNA levels of mouse MEC as in (*D*). (*H*) Nrf2 mRNA levels of COMMA-1D cells transfected with non-targeting (scramble, Scr) or mouse Nrf2 (siNrf2) siRNA oligos. Cells were analyzed at 48h post-transfection. (*I*) mRNA analysis of AhR-target Cyp1a1 in COMMA-1D cells that were transfected with single guide RNA against mouse AhR (sgAhR) and siRNA oligos specific for mouse Nrf2 (siNrf2) and then subjected to BSO (200μM) for 24h. Cells manipulated with empty vector (EV) and non-targeting (scramble, scr) siRNA were used as control. n=3/group. (*J*) mRNA levels of Ahr, CYP1A1 and CYP1A2 in the Van't Veer human BC dataset with tumors segregated by BRCA1 genotype: Wild-type, n=21; Mutated, n=18. (*K*) Inverse correlation between AhR or CYP1B1 expression with low or high BRCA1 mRNA levels in the TCGA human BC dataset.

Figure S2. **Expression of AREG in normal and malignant mammary epithelial cells and analysis of Erbb receptors and ligands.** (*A*) Immunoblot showing AREG protein in MCF10A cells that were left untreated (Ctr) or treated with 200μM BSO for 24hr or 48hr. (*B*) mRNA expression of mouse Erbb receptors as indicated in COMMA-1D cells. n=3. (*C*) mRNA expression of mouse Erbb ligands as indicated in COMMA-1D cells that were left untreated or subjected to 200 M BSO for 24h. n=3/group. (*D*) Quantification of AREG expression in BRCA1 wild-type reduction mammoplasty from healthy women used as controls, prophylactic mastectomy specimen in women heterozygous for a BRCA1

mutation (BRCA1 mutant), and human BRCA1 mutant basal/TNBC breast tumours as shown in Figure 2J.

Figure S3. **AhR-AREG axis has a pivotal role in BRCA1-associated tumorigenesis.** (*A*) mRNA levels of Nqo1 in KBP cells that were left untreated or treated with 200μM BSO for 24h. n=3/group. (*B*) Representative flow plots of DNA synthesis in KBP cells that were transfected with empty vector (EV), or vectors expressing sgAhr or sgAreg constructs, and examined at 24hr or 48hr after puromycin selection. (*C*) Representative images of EV-, sgAhr- or sgAreg- expressing KBP tumors (red arrows) in the mice on day 35 post-transplantation. (*D*) Growth curve of EV-, sgAhr- or sgAreg- expressing KBP cells by SRB colorimetric assay at different time points. (*E*) RNAseq data obtained from RNA deep sequencing of mouse MEC and KBP tumors (n=3/group). The lower and upper hinges correspond to the first and third quartiles (the 25th and 75th percentiles). The upper whisker extends from the hinge to the largest value no further than 1.5 * IQR from the hinge, and the lower whisker extends from the hinge to the smallest value at most 1.5 * IQR of the hinge (where IQR is the inter-quartile range, or distance between the first and third quartiles). (*F*) mRNA levels of Erbb ligands (Areg, Hbegf, Nrg1) in EV and sgAhR KBP tumors. n=3-5/group.

Figure S4. **Analysis of tumour-infiltrating macrophages and bone marrow derived macrophages.** (*A*,*B*) Representative plots describing the gating strategy used to characterize macrophages in the mammary fat pad of virgin and nulliparous FVB female mice and KBP mammary tumors. (*C*) Histogram of phosphorylated EGFR (p-EGFR) signal in macrophages that were positive for CD11b and F4/80 surface markers ($CD11b^+F4/80^+$) in KBP tumors. Staining with isotype control was used to assess the specificity of the signal. (*D*) Left, representative image of the concentric regions “grown” from the area and at a distance spanning from 20pix to 100pix. Right, Quantification of $CD163^+$ macrophages at different distances from an AREG-positive tumour area. (*E*) ELISA measurement of secreted VEGF-A protein in the medium of BMDM cultured alone, or after co-culture with KBP cells for 24hr (n=3/group). (*F*) Vegfa mRNA levels in KBP cells alone (-) or after co-culturing with BMDM for 24 hr. (*G*) Egfr mRNA analysis in BMDM cultured alone, or after co-culture with KBP cells for 24hr (n=3/group).

Figure S5. **Analysis of monocyte- and macrophage-related chemokines in BRCA1/p53-deleted mammary tumors.** (*A*) Levels of the indicated chemokines in the culture medium of mouse MEC or KBP cells after 24hr culture (n=4/group). (*B*) Levels of the indicated chemokines in the culture medium of EV- or sgAhr-expressing KBP cells treated for 24hr with recombinant AREG (rAREG) at 50ng/ml. (*C*) Levels of CXCL1, CXCL2 and CCL5 mRNAs in TCGA BC grouped accordingly to low or high expression of BRCA1, AhR or AREG as indicated on the x-axis (n=1102).

Figure S6. **Effect of AhR loss-of-function in human breast cancer and mouse mammary tumors.** (*A*) mRNA levels of CYP1A1 in MDA-MB-468 cell line carrying a wild-type (AhR^{wt}) or deleted form of AhR (AhR^{ko}). Cells were left untreated (Ctr) or exposed to 500 μM BSO for 24h. (*B*) Growth curve of MDA-MB-468 AhR^{wt} and AhR^{ko} cells for 4 days as measured by Tripan-blue exclusion assay. (*C*) Levels of secreted AREG in the media of the indicated cell lines that have been seeded and maintained in growth factor-rich media for 24h. (*D*,*E*) AREG levels in the culture medium of MDA-MB-468 and HCC1937 cell lines treated with increasing dose of the AhR inhibitor (AhRi), CH223191. (*F*) Immunoblot showing total EGFR, phosphorylated EGFR (P-EGFR) and AhR proteins in HCC1937 cells that were left untreated (Ctr) or treated with Erlotinib (E; 600nM) or AhRi (900nM) for 24 hr.

Figure S7. **Sensitivity of breast cancer cell lines to AhR and EGFR inhibition.** Synergy score plots as determined by analyzing data from 5-day SRB growth using the SynergyFinder web application. Red and green colors indicate the most synergistic or antagonist areas, respectively.

REFERENCES

1. Gorrini C*, et al.* (2013) BRCA1 interacts with Nrf2 to regulate antioxidant signaling and cell survival. *J Exp Med* 210(8):1529-1544.
2. Qian BZ*, et al.* (2015) FLT1 signaling in metastasis-associated macrophages activates an inflammatory signature that promotes breast cancer metastasis. *J Exp Med* 212(9):1433-1448.
3. Alexandrov LB, Nik-Zainal S, Wedge DC, Campbell PJ, & Stratton MR (2013) Deciphering signatures of mutational processes operative in human cancer. *Cell Rep* 3(1):246-259.
4. van 't Veer LJ*, et al.* (2002) Gene expression profiling predicts clinical outcome of breast cancer. *Nature* 415(6871):530-536.
5. Subramanian A*, et al.* (2005) Gene set enrichment analysis: a knowledge-based approach for interpreting genome-wide expression profiles. *Proc Natl Acad Sci U S A* 102(43):15545-15550.
6. Barbie DA*, et al.* (2009) Systematic RNA interference reveals that oncogenic KRAS-driven cancers require TBK1. *Nature* 462(7269):108-112.
7. Becht E*, et al.* (2016) Estimating the population abundance of tissue-infiltrating immune and stromal cell populations using gene expression. *Genome Biol* 17(1):218.
8. Matys V*, et al.* (2006) TRANSFAC and its module TRANSCompel: transcriptional gene regulation in eukaryotes. *Nucleic Acids Res* 34(Database issue):D108-110.
9. Barretina J*, et al.* (2012) The Cancer Cell Line Encyclopedia enables predictive modelling of anticancer drug sensitivity. *Nature* 483(7391):603-607.
10. Cancer Cell Line Encyclopedia C & Genomics of Drug Sensitivity in Cancer C (2015) Pharmacogenomic agreement between two cancer cell line data sets. *Nature* 528(7580):84-87.
11. Thu KL*, et al.* (2018) Disruption of the anaphase-promoting complex confers resistance to TTK inhibitors in triple-negative breast cancer. *Proc Natl Acad Sci U S A* 115(7):E1570-E1577.

Figure S1

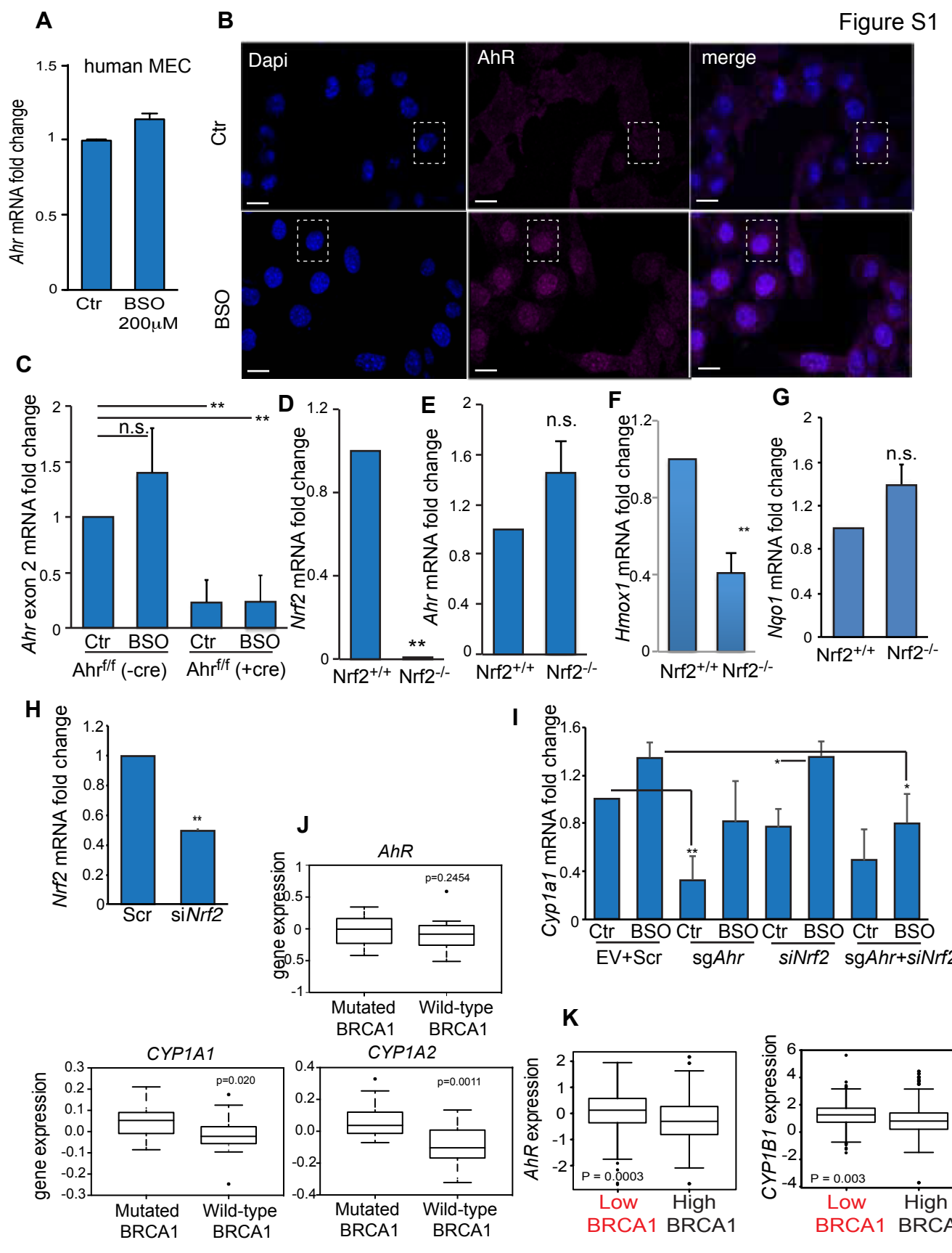
A
human MEC
Ahr mRNA fold change
Ctr
BSO 200μM
B
Dapi
AhR
merge
Ctr
BSO
C
Ahr exon 2 mRNA fold change
n.s.
**
Ctr BSO Ctr BSO
Ahr f/f (-cre)
Ahr f/f (+cre)
D
Nrf2 mRNA fold change
Nrf2 +/+
Nrf2 -/-
E
Ahr mRNA fold change
n.s.
F
Hmox1 mRNA fold change
G
Nqo1 mRNA fold change
H
Nrf2 mRNA fold change
Scr
siNrf2
I
Cyp1a1 mRNA fold change
EV+Scr
sgAhr
siNrf2
sgAhr+siNrf2
J
AhR
p=0.2454
gene expression
Mutated BRCA1
Wild-type BRCA1
CYP1A1
p=0.020
CYP1A2
p=0.0011
K
AhR expression
P = 0.0003
Low BRCA1
High BRCA1
CYP1B1 expression
P = 0.003

Figure 2

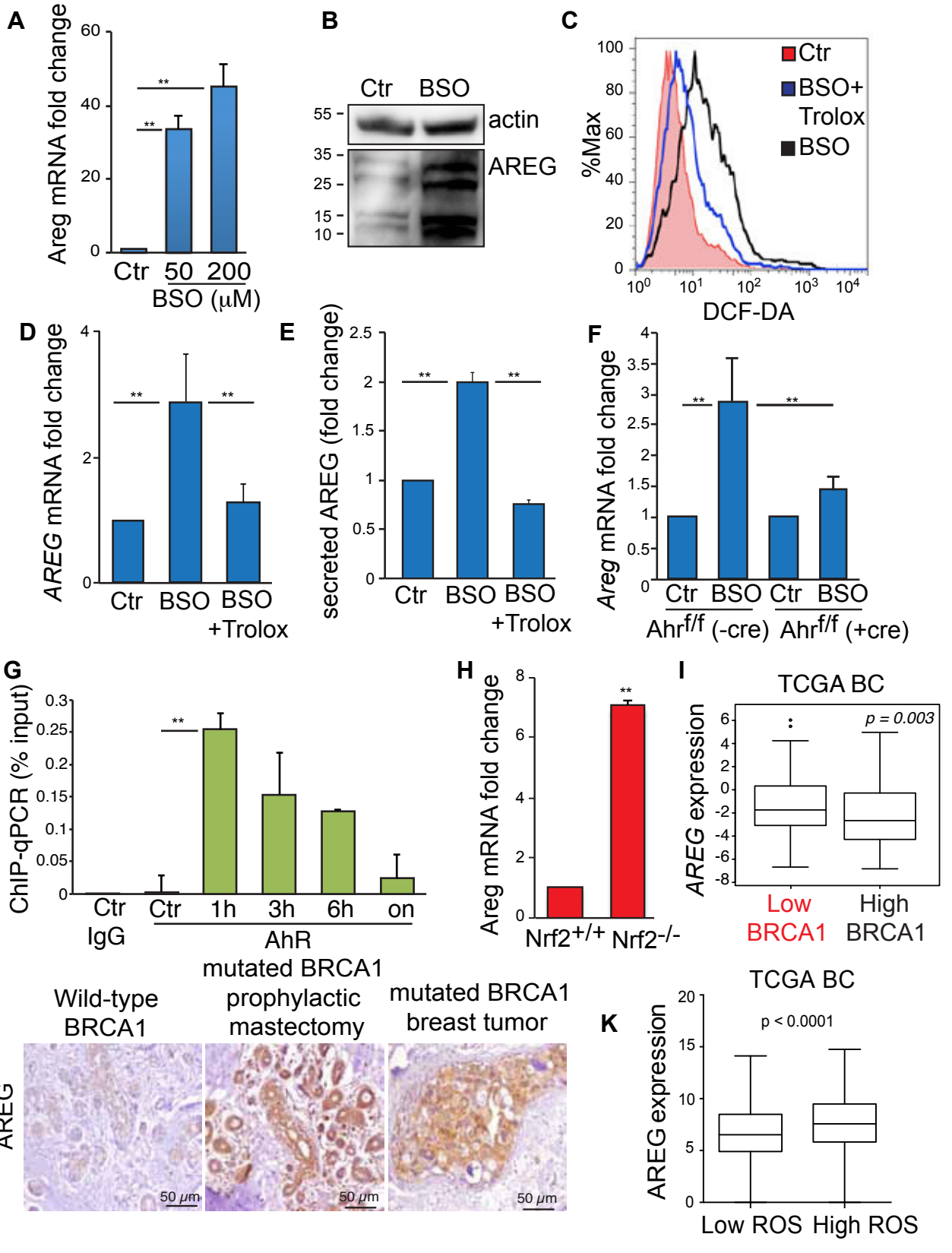
A
Areg mRNA fold change
60
40
20
0
**
**
Ctr
50
200
BSO (μM)
B
Ctr
BSO
55
35
25
15
10
actin
AREG
C
100
80
60
40
20
0
%Max
Ctr
BSO+
Trolox
BSO
10^0
10^1
10^2
10^3
10^4
DCF-DA
D
AREG mRNA fold change
4
2
0
**
**
Ctr
BSO
BSO
+Trolox
E
secreted AREG (fold change)
2.5
2
1.5
1
0.5
0
**
**
Ctr
BSO
BSO
+Trolox
F
Areg mRNA fold change
4
3.5
3
2.5
2
1.5
1
0.5
0
**
**
Ctr
BSO
Ctr
BSO
Ahr$^{f/f}$ (-cre)
Ahr$^{f/f}$ (+cre)
G
ChIP-qPCR (% input)
0.3
0.25
0.2
0.15
0.1
0.05
0
**
Ctr
IgG
Ctr
1h
3h
6h
on
AhR
H
Areg mRNA fold change
8
6
4
2
0
**
Nrf2$^{+/+}$
Nrf2$^{-/-}$
I
TCGA BC
p = 0.003
AREG expression
6
4
2
0
-2
-4
-6
-8
Low
BRCA1
High
BRCA1
J
Wild-type
BRCA1
mutated BRCA1
prophylactic
mastectomy
mutated BRCA1
breast tumor
AREG
50 μm
50 μm
50 μm
K
TCGA BC
p < 0.0001
AREG expression
20
15
10
5
0
Low ROS
High ROS

Figure S3

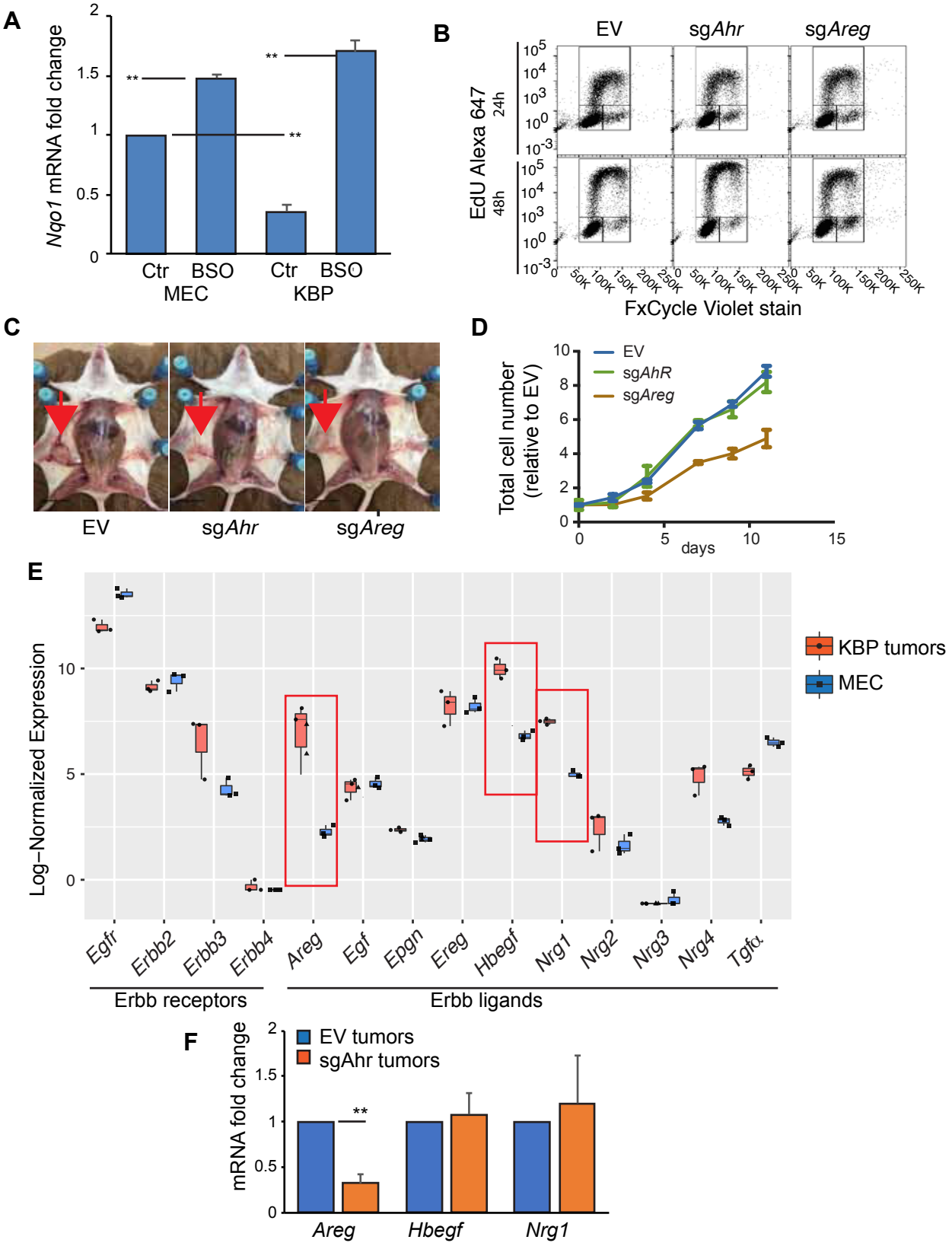
A
Nqo1 mRNA fold change
Ctr
BSO
MEC
Ctr
BSO
KBP
B
EV
sgAhr
sgAreg
EdU Alexa 647
24h
48h
FxCycle Violet stain
C
EV
sgAhr
sgAreg
D
Total cell number (relative to EV)
EV
sgAhR
sgAreg
days
E
Log−Normalized Expression
KBP tumors
MEC
Egfr
Erbb2
Erbb3
Erbb4
Areg
Egf
Epgn
Ereg
Hbegf
Nrg1
Nrg2
Nrg3
Nrg4
Tgfα
Erbb receptors
Erbb ligands
F
mRNA fold change
EV tumors
sgAhr tumors
Areg
Hbegf
Nrg1

Figure S4

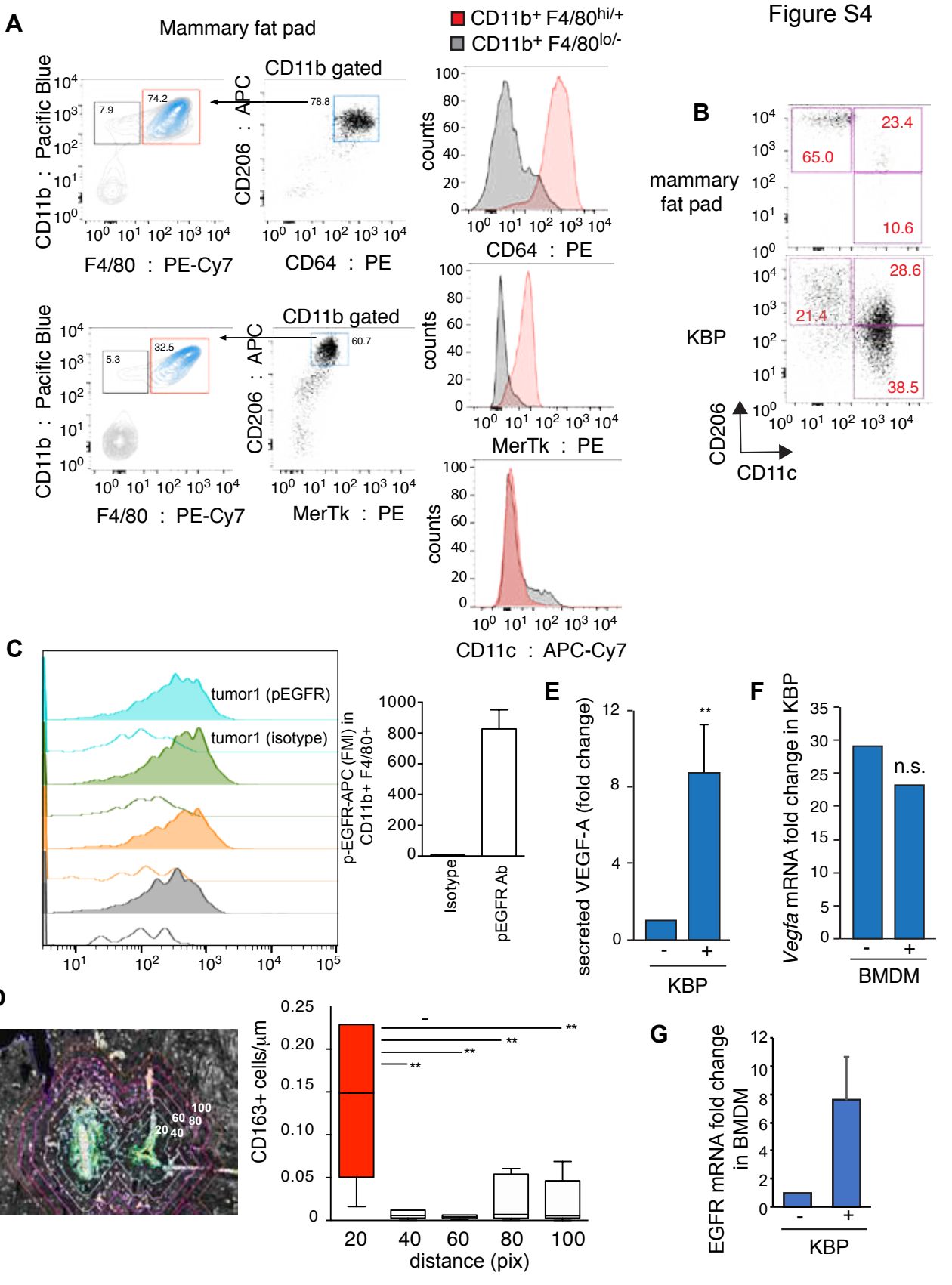
A
Mammary fat pad
CD11b+ F4/80hi/+
CD11b+ F4/80lo/-
CD11b gated
CD11b : Pacific Blue
F4/80 : PE-Cy7
CD206 : APC
CD64 : PE
MerTk : PE
counts
CD11c : APC-Cy7
B
mammary fat pad
KBP
CD206
CD11c
C
tumor1 (pEGFR)
tumor1 (isotype)
p-EGFR-APC (FMI) in CD11b+ F4/80+
Isotype
pEGFR Ab
D
CD163+ cells/µm
distance (pix)
E
secreted VEGF-A (fold change)
KBP
F
Vegfa mRNA fold change in KBP
n.s.
BMDM
G
EGFR mRNA fold change in BMDM
KBP

Figure S5

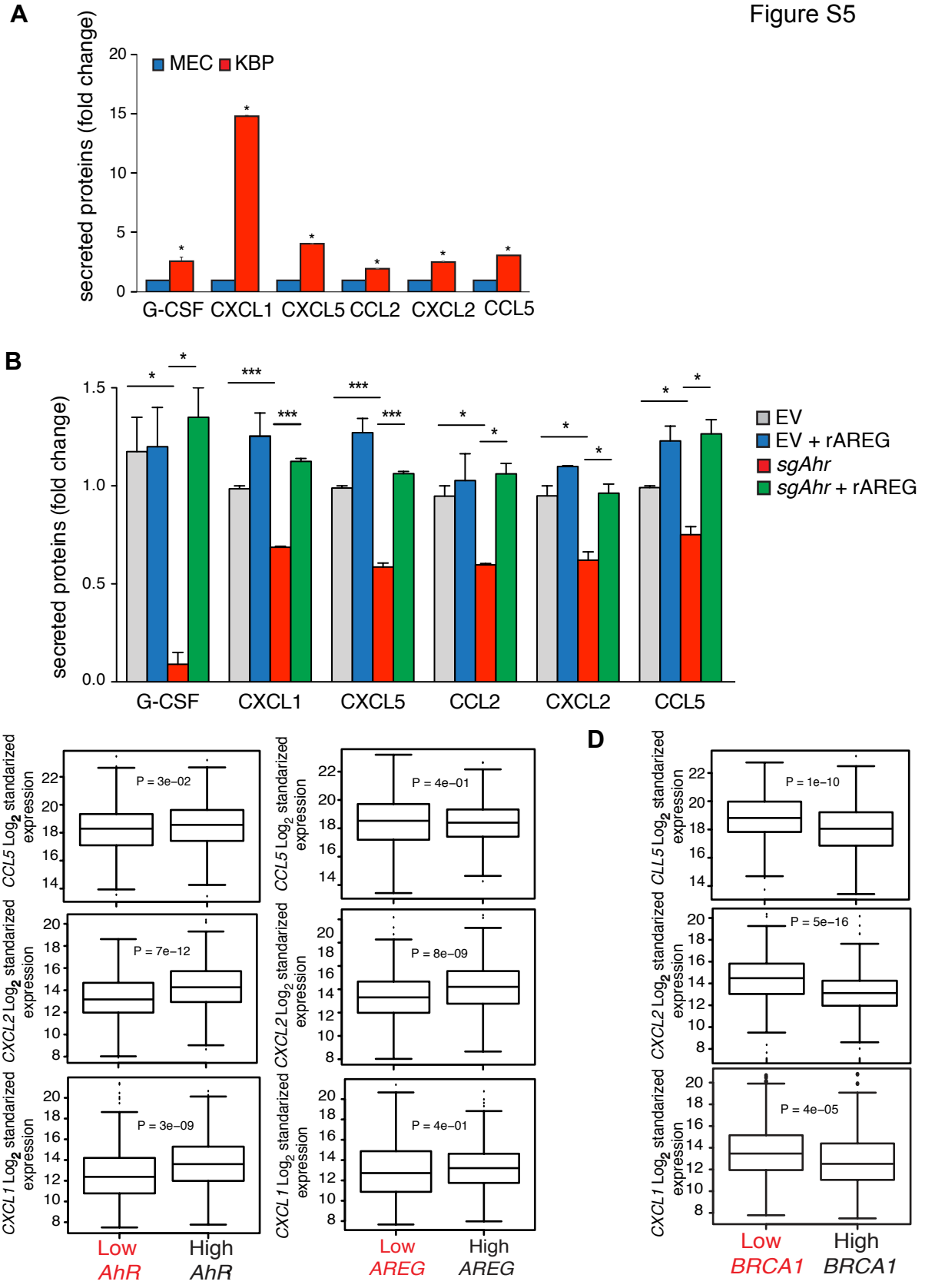
A
secreted proteins (fold change)
MEC
KBP
G-CSF
CXCL1
CXCL5
CCL2
CXCL2
CCL5
B
secreted proteins (fold change)
EV
EV + rAREG
sgAhr
sgAhr + rAREG
C
CCL5 Log2 standarized expression
CXCL2 Log2 standarized expression
CXCL1 Log2 standarized expression
P = 3e−02
P = 7e−12
P = 3e−09
P = 4e−01
P = 8e−09
P = 4e−01
Low AhR
High AhR
Low AREG
High AREG
D
CCL5 Log2 standarized expression
CXCL2 Log2 standarized expression
CXCL1 Log2 standarized expression
P = 1e−10
P = 5e−16
P = 4e−05
Low BRCA1
High BRCA1

Figure S6

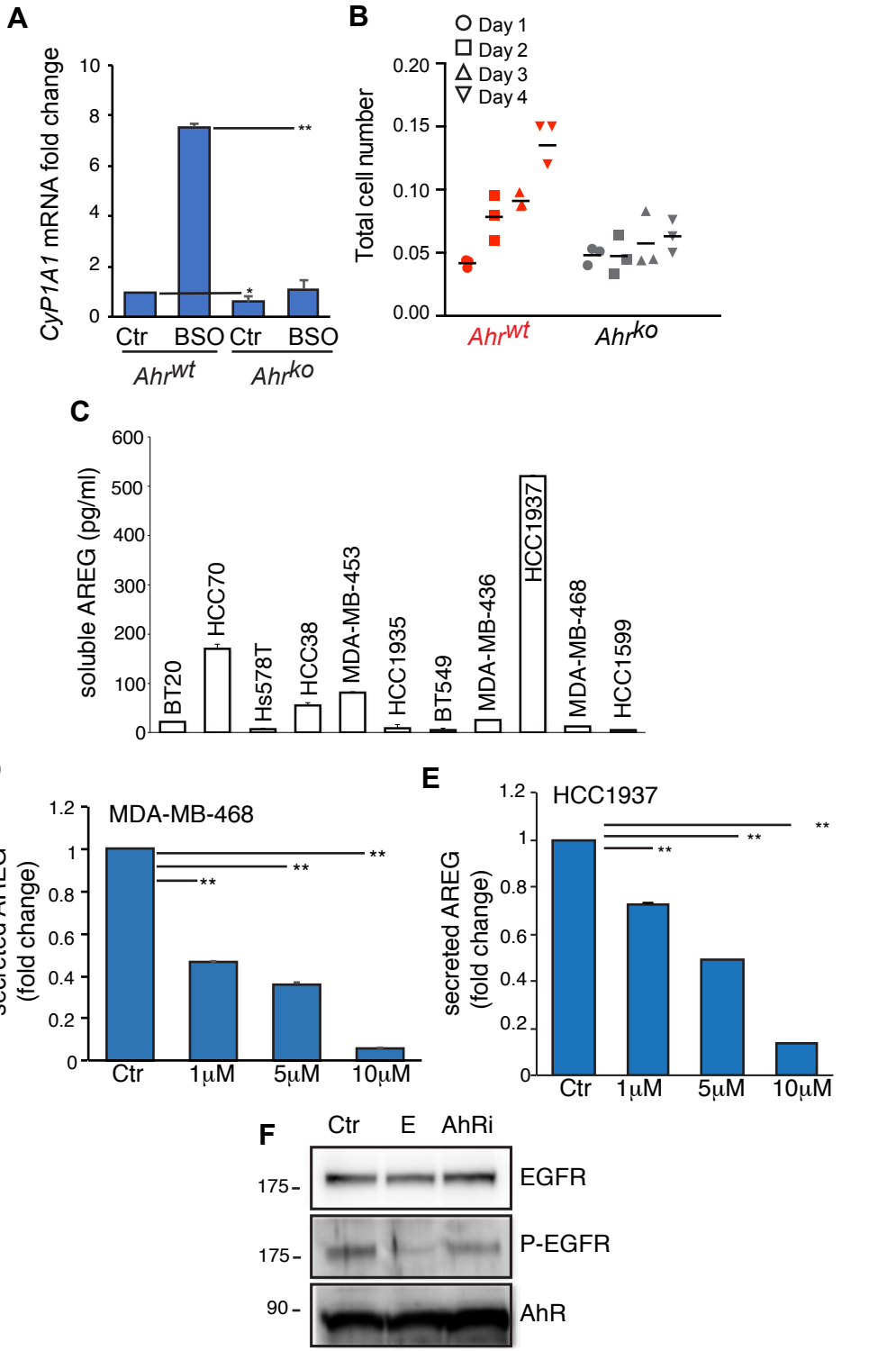
A
CyP1A1 mRNA fold change
Ctr
BSO
Ctr
BSO
Ahrwt
Ahrko
B
Day 1
Day 2
Day 3
Day 4
Total cell number
Ahrwt
Ahrko
C
soluble AREG (pg/ml)
BT20
HCC70
Hs578T
HCC38
MDA-MB-453
HCC1935
BT549
MDA-MB-436
HCC1937
MDA-MB-468
HCC1599
D
MDA-MB-468
secreted AREG (fold change)
Ctr
1μM
5μM
10μM
E
HCC1937
secreted AREG (fold change)
Ctr
1μM
5μM
10μM
F
Ctr
E
AhRi
EGFR
P-EGFR
AhR

Figure S7

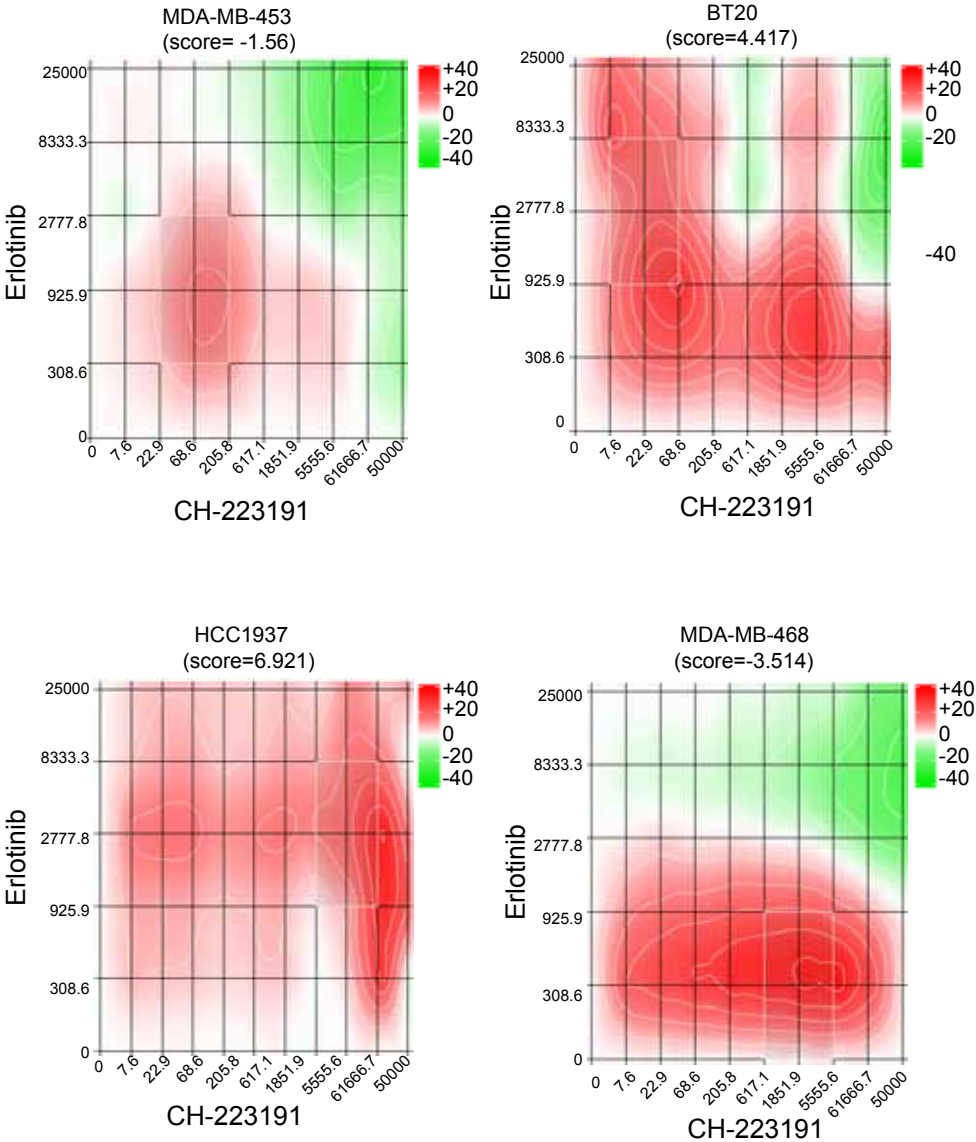
MDA-MB-453
(score= -1.56)
BT20
(score=4.417)
HCC1937
(score=6.921)
MDA-MB-468
(score=-3.514)
Erlotinib
CH-223191
25000
8333.3
2777.8
925.9
308.6
0
7.6
22.9
68.6
205.8
617.1
1851.9
5555.6
61666.7
50000
+40
+20
0
-20
-40

Supplementary Table 1: Primers used for qRT-PCR (m=mouse)

Gene	**Primer Sequence**
mRps9 F	GCAAGATGAAGCTGGATTAC
mRps9 R	GGGATGTTCACCACCTG
mNqo1 F	AGGATGGGAGGTACTCGAATC
mNqo1 R	AGGCGTCCTTCCTTATATGCTA
mHmox1 F	AAGCCGAGAATGCTGAGTTCA
mHmox1 R	GCCGTGTAGATAATGGTACAAGGA
mCypya1-F	CTCTTCCCTGGATGCCTTCAA
mCypya1-R	GGATGTGGCCCTTCTCAAATG
mAreg-F	GGTCTTAGGCTCAGGCCATT
mAreg-R	AGAGTTCACTGCCAGAAGGC
mAhr-F	CGGAGCGCTGCTTCCTCCAC
mAhr-R	GCTGCCCTTTGGCATCACAACC
mEgf-F	AGGATCCTGACCCCGAACTT
mEgf-R	ACAGCCGTGATTCTGAGTGG
mEpgn-F	TGGCTCTGGGGGTTCTGATA
mEpgn-R	TGTAGTCAGCTTCGGTGTTGT
mEreg-F	TGCTTTGTCTAGGTTCCCACC
mEreg-R	CGGGGATCGTCTTCCATCTG
mHbegf-F	TTTCTGGCCGCAGTGTTGTC
mHbegf-R	GTGGGTAGCAGCTGGTTTGT
mNrg1-F	GCAAAGAAGGCAGAGGCAAG
mNrg1-R	AATCTGGGAGGCAATGCTGG
mNrg2-F	CACTCTGTCATCCTGGTCGG
mNrg2-R	TCAGCCTTTTGCTTAGGATCTGG
mNrg3-F	CCTATCAAGCACCACAGCCC
mNrg3-R	CCTGACCTCTATCCCTTGGC
mNrg4-F	TACGACGAGAGAAGTCCCAG
mNrg4-R	TAGCAGGGTGCAAGGTCAAC
mTgf_alpha_F	TAGCGCTGGGTATCCTGTTAG
mTgf_alpha_R	GAGTGTGGGAATCTGGGCAC
mEgfr-F	CACGCCAACTGTACCTATGGATGT
mEgfr-R	GGCCCAGAGGATTTGGAAGAA
mErbb2-F	GGCACTGTCTACAAGGGCAT
mErbb2-R	GAGGCGGGACACATATGGAG
mErbb3-F	CACCCAAGGGTGTAAGGGAC
mErbb3-R	CGCTCCAAGTAGCGTCTCAT
mErbb4-F	GGACGGGCCATTCCACTTTA
mErbb4-R	AAGGGCTCTACCAGCTCTGT

SI Appendix Table 2: Primers used for ChIP-qPCR (m=mouse)

mAreg_XRE_F	ttctccccgcgtaatcagg
mAreg_XRE_R	gccgggaggttactactccaa
mCyp1a1_XRE_F	caggcaacacagagaagtcg
mCyp1a1_XRE_R	aagcatcacccttgtagcc